






Article

# New Series of Double-Modified Colchicine Derivatives: Synthesis, Cytotoxic Effect and Molecular Docking

Julia Krzywik <sup>1,2</sup>, Maral Aminpour <sup>3</sup>, Ewa Maj <sup>4</sup>, Witold Mozga <sup>2</sup>, Joanna Wietrzyk <sup>4</sup>, Jack A. Tuszyński <sup>3,5</sup> and Adam Huczynski <sup>1,\*</sup>

<sup>1</sup> Department of Medical Chemistry, Faculty of Chemistry, Adam Mickiewicz University, Uniwersytetu Poznańskiego 8, 61-614 Poznań, Poland; julia.krzywik@amu.edu.pl

<sup>2</sup> TriMen Chemicals, Piłsudskiego 141, 92-318 Łódź, Poland; mozga@trimen.pl

<sup>3</sup> Department of Oncology, University of Alberta, Edmonton, AB T6G 1Z2, Canada; aminpour@ualberta.ca (M.A.); jack.tuszynski@gmail.com (J.A.T.)

<sup>4</sup> Hirsfeld Institute of Immunology and Experimental Therapy, Polish Academy of Sciences, Rudolfa Weigla 12, 53-114 Wrocław, Poland; ewa.maj@hirsfeld.pl (E.M.); joanna.wietrzyk@hirsfeld.pl (J.W.)

<sup>5</sup> DIMEAS, Politecnico di Torino, Corso Duca degli Abruzzi, 24, 10129 Torino, Italy

\* Correspondence: adhucz@amu.edu.pl; Tel.: +48-61-8291673

Academic Editors: Bartosz Tylkowski, Anna Bajek and Krzysztof Roszkowski

Received: 14 July 2020; Accepted: 31 July 2020; Published: 2 August 2020

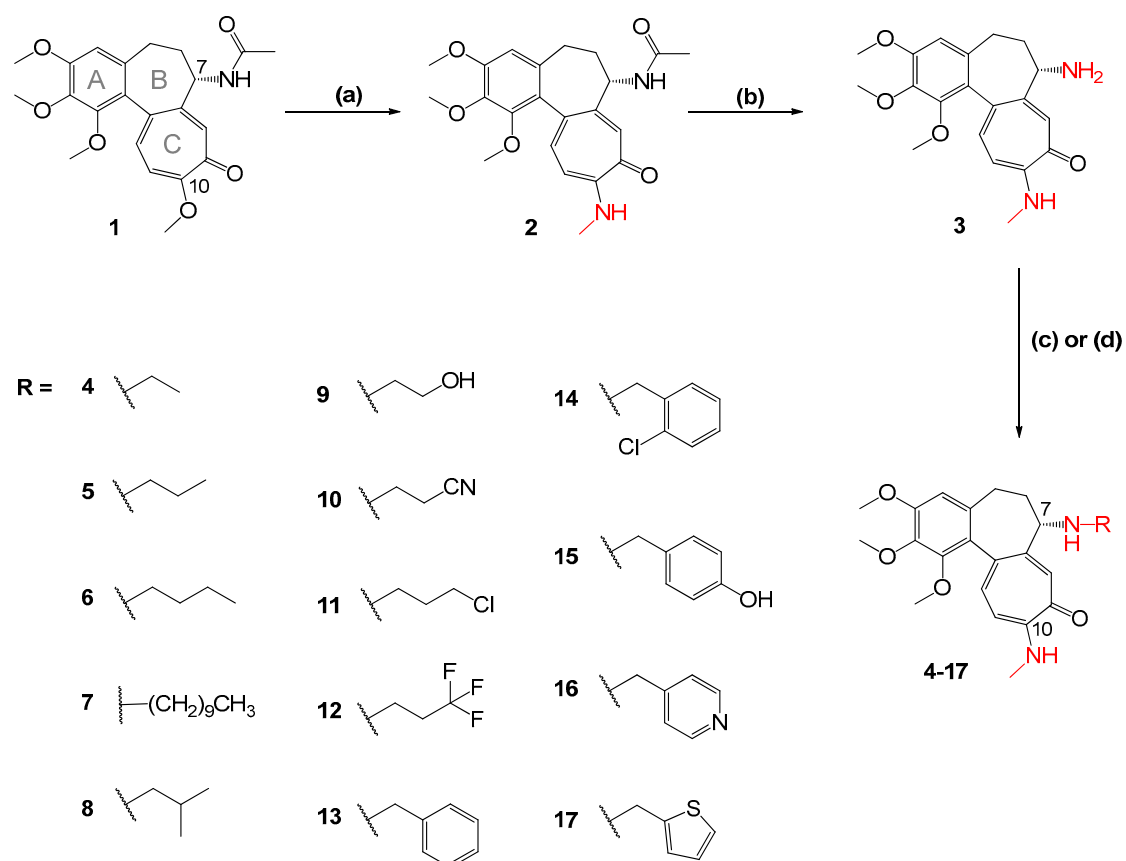


**Abstract:** Colchicine is a well-known anticancer compound showing antimitotic effect on cells. Its high cytotoxic activity against different cancer cell lines has been demonstrated many times. In this paper we report the syntheses and spectroscopic analyses of novel colchicine derivatives obtained by structural modifications at C7 (carbon-nitrogen single bond) and C10 (methylamino group) positions. All the obtained compounds have been tested *in vitro* to determine their cytotoxicity toward A549, MCF-7, LoVo, LoVo/DX, and BALB/3T3 cell lines. The majority of obtained derivatives exhibited higher cytotoxicity than colchicine, doxorubicin and cisplatin against the tested cancerous cell lines. Additionally, most of the presented derivatives were able to overcome the resistance of LoVo/DX cells. Additionally, their mode of binding to  $\beta$ -tubulin was evaluated *in silico*. Molecular docking studies showed that apart from the initial amides **1** and **2**, compound **14**, which had the best antiproliferative activity ( $IC_{50} = 0.1\text{--}1.6$  nM), stood out also in terms of its predicted binding energy and probably binds best into the active site of  $\beta$ 1-tubulin isotype.

**Keywords:** anticancer agents; colchicine derivatives; reductive alkylation; tubulin inhibitors; docking studies

## 1. Introduction

Tubulin is the target of some of the most widely used anticancer anti-mitotic agents, such as vinblastine or paclitaxel [1,2]. Unfortunately, clinical usefulness of many microtubule disrupting agents has been reduced as a result of tumor cell multidrug-resistance (MDR). The main role in MDR is played by P-glycoprotein, which is overexpressed in various types of cancers and is known to be associated with poor response to chemotherapy [3–5]. Colchicine **1** (see Scheme 1) is a plant-based alkaloid extracted from *Colchicum autumnale* and *Gloriosa superba* that shows antimitotic effects on a number of cancer cell lines. It binds to tubulin, inhibiting its assembly and microtubule polymerization and finally arresting cell division at metaphase [6–12]. However, in addition to the problem with cancer cells developing drug resistance, colchicine was found to have some toxic effects, including accumulation in the gastrointestinal tract, as well as neurotoxicity [6,13–19]. These are the two main disadvantages that limit the use of colchicine in chemotherapy.



**Scheme 1.** Synthesis of double-modified colchicine derivatives (2–17), changes at C7 and C10 positions are highlighted in red. Reagents and conditions: (a)  $\text{NHCH}_3/\text{EtOH}$ , reflux; (b) 2M HCl, reflux; (c) respective aldehyde,  $\text{NaBH}_3\text{CN}$ , MeOH, RT for 4–9 and 11–17; (d) acrylonitrile, MeOH, RT for 10.

Despite the above limitations, colchicine exhibits high antiproliferative activity and represents an interesting research area for understanding of relationship between the structure and biological activity (SAR) of compounds interacting with tubulin. Many colchicine analogues containing amide or urethane at position C7 have been studied [20–27]. Such groups may be hydrolyzed *in vivo* causing a change in pharmacological activity [28,29]. Conversion of such moieties into single carbon-nitrogen bond prevents hydrolysis of the side chain in the cells and creates a new class of colchicine derivatives. Numerous modified colchicine and thiocolchicine derivatives with substituted benzyl moieties at carbon C7 have been synthesized and their biological activity has been evaluated. Some of the described derivatives showed antiproliferative activity superior to that of colchicine [22,30]. In addition, as shown in our earlier studies, the replacement of  $-\text{OCH}_3$  group at position C10 with  $-\text{NHCH}_3$  group leads to generation of compounds more active than unmodified colchicine [20]. On the basis of these findings, we decided to develop the concept, design, and synthesize a new series of double-modified colchicine derivatives with different amine moieties at C7 atom (aromatic but also alkyl substituents that have not been previously widely studied) and with a methylamino group at C10 atom in the tropolone ring C.

Herein, we report the syntheses and spectroscopic analyses of a series of structurally different derivatives of colchicine obtained by its modification at C7 (amide bond replacement by a carbon-nitrogen single bond) and C10 (methylamino group) positions. We also describe the results of *in vitro* antiproliferative activity evaluation of the starting compounds 1–2 and the obtained colchicine derivatives (3–17) against four human cancer cell lines, namely A549, MCF-7, LoVo, and LoVo/DX as well as normal murine cells BALB/3T3. To gain more knowledge about molecular mechanism of action of the investigated compounds (1–17), we also present *in silico* results of a molecular docking

study into the colchicine-binding site (CBS) of  $\beta$ -tubulin. The derivatives presented in this work are double-modified colchicine derivatives with the amine groups at C7 and C10 positions. On the basis of the obtained preliminary structure–activity relationship (SAR) studies, we will be able to design new promising compounds for more extended research.

## 2. Results and Discussion

### 2.1. Chemistry

To determine the effect of replacement of the amide moiety at position C7 by a single nitrogen-carbon bond and, at the same time,  $-\text{OCH}_3$  group replacement by  $-\text{NHCH}_3$  at position C10 of colchicine **1**, on its bioactivity, fourteen new derivatives (**4–17**) were designed. The obtained compounds contained different moieties (replacing acetamide of unmodified compound **1**) attached to nitrogen at position C7, such as: alkyl chains of various length, straight or branched (**4–8**), alkyl chains containing various substituents (**9–12**), aromatic moiety with or without substituents (**13–15**) or with heteroatom in the ring (**16–17**). Diversity of groups at position C7 is intended to facilitate the analysis of the structure–activity relationship. The synthetic routes to colchicine derivatives **2–17** are outlined in Scheme 1.

Compound **3** was readily available from **1** by treatment with methylamine and followed by hydrolysis with 2M HCl [20,31]. *N*-deacetyl-10-methylamino-10-demethoxycolchicine **3** became the starting material for the synthesis of new derivatives (**4–17**). On the basis of the method described previously [22], reductive alkylation of **3** in a reaction with the corresponding aldehyde in the presence of sodium cyanoborohydride allowed us to obtain double-modified compounds **4–9** and **11–17**. However, aldehydes used in the present paper did not require activation with acid, so the reactions were carried out without the addition of acetic acid, which eliminated the formation of unidentified by-products. Most of the aldehydes necessary for the synthesis of the designed compounds were purchased, but aldehydes for the synthesis of compounds **4** and **11** were obtained by oxidation of the corresponding alcohols using pyridinium chlorochromate, PCC [32]. Compound **10** was synthesized via addition of amine (**3**) to the Michael acceptors (acrylonitrile). All obtained compounds (**2–17**) were isolated in pure form after column flash chromatography on silica gel.

The structures and purities of all products **2–17** were determined using the LC-MS,  $^1\text{H}$  and  $^{13}\text{C}$  NMR analyses, and are shown in Supplementary Materials and discussed below. The signals corresponding to  $-\text{OCH}_3$  group at position C10 of **1** in the  $^1\text{H}$  NMR and  $^{13}\text{C}$  NMR spectra were observed as singlets at 4.0 ppm and at 56.5 ppm, respectively. After replacement of this group in the tropolone ring of colchicine by  $-\text{NHCH}_3$  group in compounds **2–17**, new signals appeared, at 3.0–3.1 ppm as a doublet and 7.2–7.3 ppm as a quartet in  $^1\text{H}$  NMR spectra and at 29.5–29.9 ppm in  $^{13}\text{C}$  NMR spectra. The signals characteristic of the acetyl group in colchicine **1** appeared at 1.9 ppm ( $-\text{CH}_3$ ) and 8.6 ppm ( $-\text{NH}-$ ) in  $^1\text{H}$  NMR and at 22.7 ppm ( $-\text{CH}_3$ ) and 170.3 ppm ( $-\text{C}=\text{O}$ ) in  $^{13}\text{C}$  NMR, respectively. These signals are no longer observed in the NMR spectra of **3–17** derivatives. The signal assigned to the hydrogen atom at C7 has been shifted from 4.6 ppm for unmodified colchicine **1** to 3.4–3.6 ppm for compounds **3–17**. The ESI mass spectrometry confirmed the structure of the obtained analogs by the presence of  $m/z$  signals assigned to the corresponding pseudomolecular ions of these compounds.

### 2.2. In Vitro Determination of Drug-Induced Inhibition of Human Cancer Cell Line Growth

The tested compounds (**1–17**) were evaluated for their in vitro antiproliferative effect on four human cancer cell lines and one normal murine embryonic fibroblast cell line according to the previously published procedure [20]. Detailed information concerning antiproliferation assay can be found in Supplementary Materials.

All obtained derivatives showed better antiproliferative activity than those of the commonly used antitumor agents doxorubicin and cisplatin. It is also worth noting that all compounds (except **7** with

long alkyl chain) were characterized by very high cytotoxicity with  $IC_{50} \leq 10$  nM towards three of the four tumor lines tested (see Table 1).

**Table 1.** Antiproliferative activity ( $IC_{50}$ ) [nM] of colchicine (1) and its derivatives (2–17) compared with that of standard anticancer drugs doxorubicin and cisplatin.

Compound	A549	MCF-7	LoVo	LoVo/DX	BALB/3T3
	$IC_{50}$ [nM]	$IC_{50}$ [nM]	$IC_{50}$ [nM]	$IC_{50}$ [nM]	$IC_{50}$ [nM]
1	45.2 ± 18.6	10.9 ± 0.9	9.9 ± 1.0	702.2 ± 38.2	33.1 ± 16.0
2	7.2 ± 1.3	1.6 ± 0.5	1.2 ± 0.2	80.6 ± 18.7	7.5 ± 1.0
3	8.6 ± 3.9	9.8 ± 4.5	7.4 ± 2.7	39.5 ± 18.6	7.1 ± 3.6
4	9.4 ± 3.2	8.7 ± 3.3	7.3 ± 2.5	62.0 ± 7.5	8.0 ± 1.6
5	10.5 ± 0.7	10.4 ± 0.6	5.0 ± 0.1	17.2 ± 6.7	8.6 ± 0.4
6	8.1 ± 2.6	8.7 ± 3.1	7.8 ± 1.3	13.3 ± 5.8	7.5 ± 1.6
7	88.4 ± 3.2	75.2 ± 10.8	46.6 ± 15.5	99.5 ± 35.5	70.4 ± 1.2
8	9.6 ± 1.3	9.7 ± 1.5	7.8 ± 1.0	8.5 ± 1.1	7.5 ± 1.5
9	9.2 ± 2.2	10.1 ± 1.2	5.6 ± 1.5	132.0 ± 37.5	8.2 ± 0.9
10	9.0 ± 1.0	7.5 ± 0.7	2.0 ± 0.6	51.5 ± 8.6	6.7 ± 1.3
11	8.4 ± 2.2	7.6 ± 2.8	1.3 ± 0.3	12.8 ± 3.3	5.9 ± 2.5
12	9.5 ± 0.2	9.0 ± 1.7	2.3 ± 1.3	8.2 ± 0.6	7.9 ± 0.4
13	4.6 ± 1.8	7.3 ± 4.4	0.9 ± 0.4	6.0 ± 0.8	6.2 ± 0.7
14	1.1 ± 0.7	0.7 ± 0.4	0.1 ± 0.02	1.6 ± 1.0	4.5 ± 2.7
15	8.9 ± 1.4	8.5 ± 0.9	5.2 ± 0.5	72.2 ± 12.5	7.3 ± 0.7
16	8.9 ± 1.7	9.6 ± 1.8	5.2 ± 1.9	48.1 ± 14.5	6.9 ± 1.3
17	9.4 ± 0.5	9.3 ± 0.6	0.9 ± 0.3	7.9 ± 1.0	4.9 ± 2.8
Doxorubicin	172.0 ± 58.0	131.5 ± 63.7	83.2 ± 61.1	4814.7 ± 1996.9	32.3 ± 28.6
Cisplatin	4916.9 ± 1852.4	5812.2 ± 2610.6	5463.2 ± 1412.4	5013.9 ± 1562.2	3968.8 ± 995.1

The  $IC_{50}$  value is defined as the concentration of a compound at which 50% growth inhibition is observed. The  $IC_{50}$  values shown are mean ± SD. Human lung adenocarcinoma (A549), human breast adenocarcinoma (MCF-7), human colon adenocarcinoma cell line (LoVo), and doxorubicin-resistant subline (LoVo/DX), normal murine embryonic fibroblast cell line (BALB/3T3).

Even though compound 7 has a weak potential compared to the other derivatives with an amine moiety on C7 carbon and methylamino group on C10 carbon, its  $IC_{50}$  values were in the nanomolar range. The activities of the remaining derivatives against A549 cells were better than that of colchicine 1 and for the majority of compounds comparable with the second starting compound 10-methylaminocolchicine 2. Compounds 13 ( $IC_{50} = 4.6$  nM) and 14 ( $IC_{50} = 1.1$  nM) were characterized by the lowest  $IC_{50}$  values towards the A549 line. In relation to the MCF-7 cell line, the newly designed derivatives (4–17) showed activities similar to that of colchicine 1 and only one compound—a derivative with a 2-chlorobenzyl moiety 14—stood out from them having a lower  $IC_{50} = 0.7$  nM, comparable with that of amide 2 ( $IC_{50} = 1.6$  nM). In relation to the LoVo cells, most of the new derivatives exhibited higher activities than unmodified colchicine 1, and five of them had  $IC_{50}$  comparable to amide 2. Derivative 14 turned out to be the most cytotoxic towards the LoVo cell line ( $IC_{50} = 0.1$  nM). As many as five of the obtained derivatives (8, 12–14 and 17) exhibited  $IC_{50} \leq 10$  nM towards LoVo/DX cells. Moreover, compound 14 ( $IC_{50} = 1.6$  nM) was observed to be the most active towards the doxorubicin-resistant subline LoVo/DX, approx. 440 times more potent than unmodified colchicine 1 ( $IC_{50} = 702.2$  nM). Comparison of the results for C7-amine double-modified analogues and those of previously published studies of C7-amide double-modified analogues [20] showed that in both cases some of the most cytotoxic compounds were derivatives containing a 2-chlorobenzyl ring at position C7. These results are noteworthy and suggest that extended and more detailed research is necessary to determine the meaning and role of the above mentioned substituent. Additionally, it should be mentioned that the antiproliferative activity depends on the type of the tested cell lines and is different for different cells. In vitro tests allow the initial determination of biological activity, but in vivo studies are necessary to determine the therapeutic potential.

Selectivity index (SI) is a major challenge in drug discovery, because it defines the ability of a particular compound to preferentially kill tumor cells in relation to normal cells. Therefore, the obtained compounds were tested not only against cancerous cells but also against the normal murine embryonic fibroblast cell line (BALB/3T3). The majority of the tested derivatives were characterized with low SI values (see Figure 1), smaller than those found for the starting compounds 1–2. However, derivative 14 (with 2-chlorobenzyl moiety at C7 carbon), which stands out from the obtained compounds is noteworthy. Its SI values were especially high for all tested cancer cell lines (SI = 4.1 for A549 cells, SI = 6.1 for MCF-7 cells, SI = 93.7 for LoVo cells, SI = 2.8 for LoVo/DX cells) and were higher than SI of parental amides 1 and 2. *N*-(2-chlorobenzyl)-10-methylaminocolchicine 14 therefore emerges as a very promising molecule (the lowest IC<sub>50</sub> and the highest SI) for further more detail research (in vitro but also in vivo) as a potential anticancer agent. Moreover, compounds 10–13 and 17 exhibited SI > 3 for LoVo cells. The results indicated that conversion of acetyl at C7 atom of the starting compounds 1 and 2 into a single carbon-nitrogen bond did not bring (except the derivatives mentioned above, in particular 14) more selective compounds in relation to the cancer cells tested.

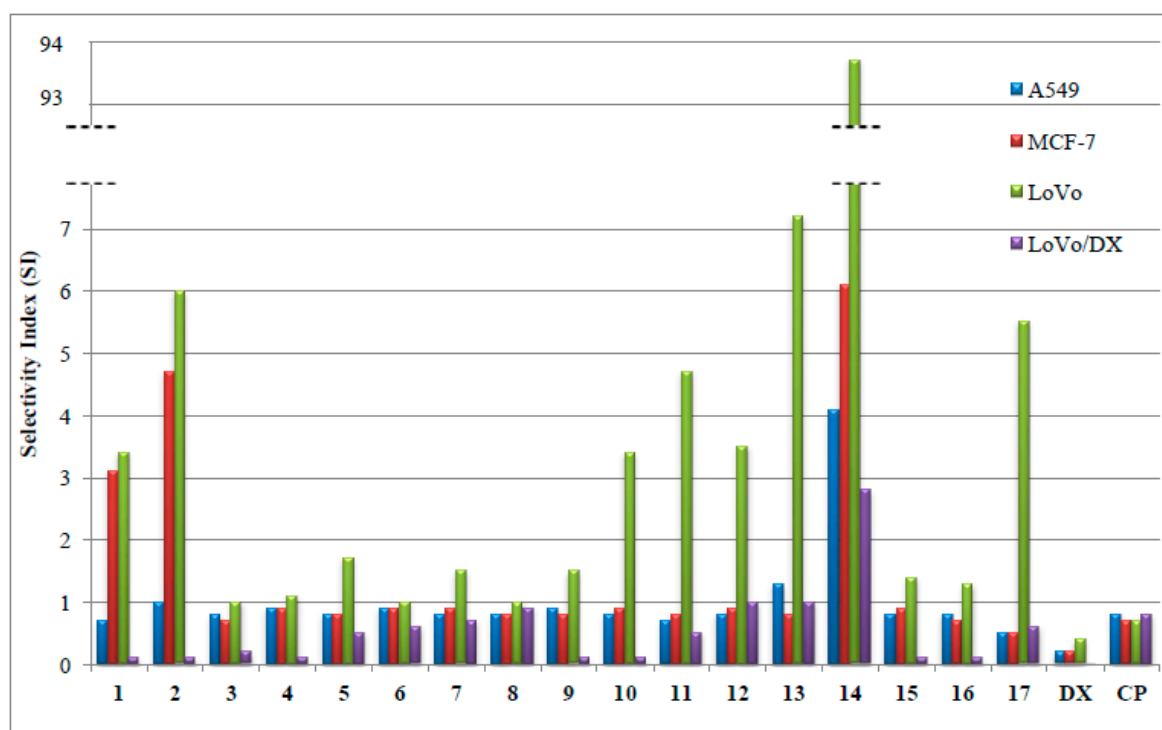


**Figure 1.** Comparison of selectivity index (SI) values of the tested compounds. The SI (Selectivity Index) was calculated for each compound using the formula:  $SI = (IC_{50} \text{ for normal cell line BALB/3T3}) / (IC_{50} \text{ for respective cancerous cell line})$ . A favorable SI > 1.0 indicates a drug with efficacy against tumor cells greater than the toxicity against normal cells.

The data presented in Table 1 show that the studied compounds inhibited the proliferation of the doxorubicin-resistant subline LoVo/DX less effectively than that of the sensitive LoVo cell line. However, all new derivatives 3–17 exhibited lower RI than the starting compounds 1 and 2 with an acetyl at position C7. In addition, as many as eleven of the tested colchicine derivatives (3–8, 11–13, 16–17) showed RI ≤ 10 (see Figure 2). The best values of the calculated resistance index, RI = 1.1–2.1 were obtained for derivatives 6–8 (*N*-butyl/*N*-decyl/*N*-isobutyl 10-methylaminocolchicine), which means that the cells are very sensitive to these compounds. The results indicate that some of the double-modified colchicine derivatives are able to overcome the drug resistance of the LoVo/DX cell line, but this desirable property was offset by poor SI values (see Figure 1). It is possible that a replacement of the amide moiety at position C7 by a single nitrogen-carbon bond will solve one of

the main problems of using colchicine in chemotherapy (multidrug resistance) and therefore, such derivatives should be taken into account for further investigation aimed at structure optimization.

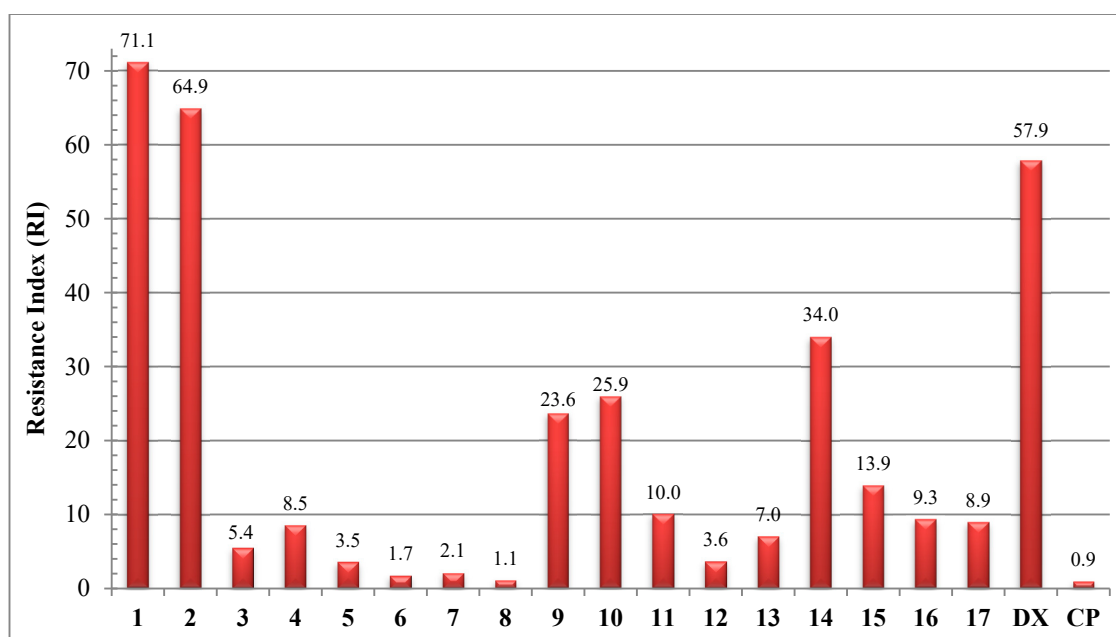


**Figure 2.** Comparison of resistance index (RI) values of tested compounds. RI indicates how many times more chemoresistant is a resistant subline relative to its parental cell line. The RI was calculated for each compound using the formula:  $RI = (IC_{50} \text{ for LoVo/DX}) / (IC_{50} \text{ for LoVo})$  cell line. When RI is 0–2, the cells are sensitive to the compound tested, RI in the range 2–10 means that the cell shows moderate sensitivity to the drug tested, RI above 10 indicates strong drug resistance.

### 2.3. *In Silico* Determination of the Molecular Mode of Action

In our study, computational methodology (according to the previously published procedure [20]) has been employed to precisely explore the molecular basis for the binding of the fourteen novel colchicines to  $\beta$ -tubulin. The  $\beta$ -tubulin monomer together with the highly homologous  $\beta$ -tubulin monomer form a stable dimer, which is the building block of microtubules in the cytoskeleton structure of every eukaryotic cell. Tubulin, in particular  $\beta$ -tubulin, is the target of many antiproliferative agents. In our simulations, compounds described above were docked into the most abundant isotype of  $\beta$ -tubulin in most cancer cells ( $\beta$ I-tubulin) in the colchicine-binding site and ranked according to their predicted binding affinity.

According to our computational predictions, the compounds from the lowest binding energy to the highest are ordered as follows: **1** (−39.1), **2** (−37.5), **14** (−31.5), **16** (−27.4), **15** (−27.1), **11** (−19.9), **6** (−19.4), **4** (−17.2), **7** (−16.9), **5** (−4.9), **3** (−4.5), **17** (−3.6), **9** (−2.6), **8** (−1.0), **10** (5.0), and **12** (8.7) with the binding energies in the parentheses given in kcal/mol units. Binding energies of these compounds are shown in Figure 3 and in Supplementary Materials Table S1.



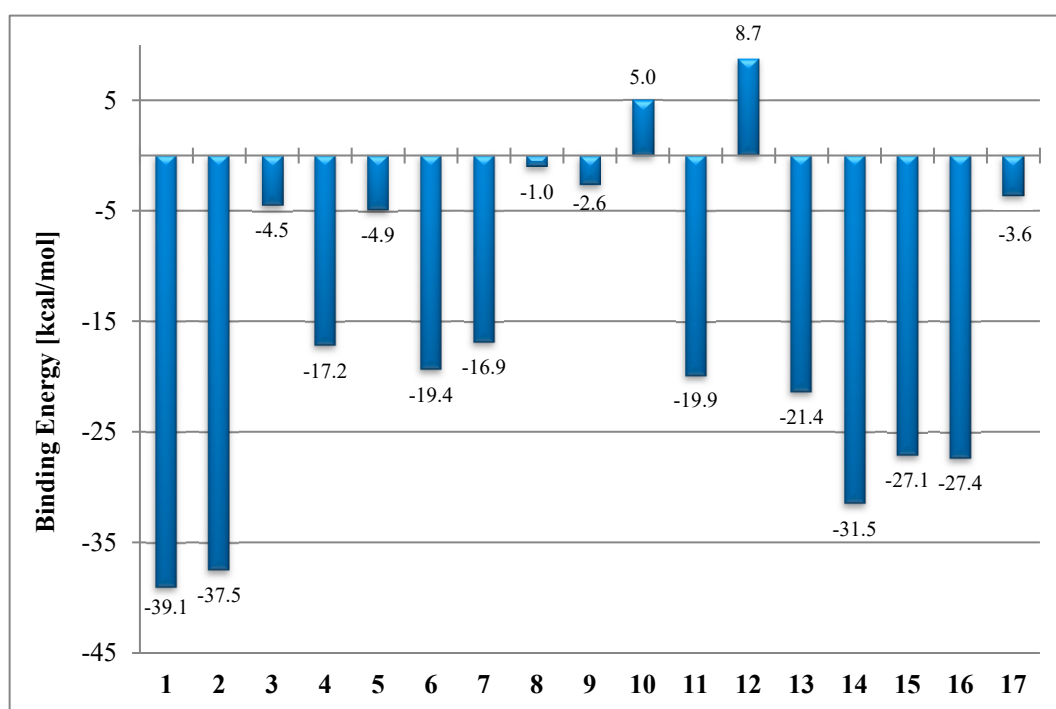


**Figure 3.** Comparison of binding energies of the tested compounds complexed with tubulin  $\beta$ 1. Binding energies are estimated using the molecular mechanics generalized Born/surface area (MM/GBSA) method.

Replacement of the methoxy group in colchicine **1** by the methylamino group in derivative **2** at C10 carbon significantly improved the antiproliferative activity of unmodified **1** (Table 1) but their BE values did not differ significantly ( $-39.1$  kcal/mol for **1** and  $-37.5$  kcal/mol for **2**). Compound **14** was the most toxic to tumor cells ( $IC_{50} = 0.1$ – $1.6$  nM) and has the third lowest energy ( $-31.5$  kcal/mol). These observations may indicate that the new double-modified colchicine **14** fits well to  $\beta$ I-tubulin and may have a similar mechanism of action to **1**, despite significantly lower  $IC_{50}$  values. However, if we look at subsequent derivatives with a relatively low BE, **15**–**16** (approx.  $-27.0$  kcal/mol) close to BE for **14** and compare with their  $IC_{50}$  values, we notice here the absence of any correlation—compounds **15** and **16** were definitely less active in vitro than compound **14**. In turn, compounds **5**, **8**–**10**, **12** and **17** had the highest BE from among the new derivatives with a single carbon-nitrogen bond at position C7 (**4**–**17**) even though their  $IC_{50}$  values were comparable or lower than those of compounds **15** and **16** with low binding energies. Thus, the trend in the computed binding energy values is not the same as for  $IC_{50}$  values that were determined from the experimental assays. However, it should be emphasized that  $IC_{50}$  is strongly dependent on the ability of these compounds to enter cancer cells through their membranes without being removed by efflux pumps and cause cell death. Since there is little correlation here, we conclude that this ability depends mainly on: solubility and membrane permeability plus affinity to P-glycoproteins (P-gp). It is worth mentioning that colchicine is subject to multidrug resistance in tumor cells as a P-gp substrate. It induces P-gp activity causing a conformational change, which subsequently leads to its rapid efflux from tumor cells [4,33,34]. Binding energy to its primary target, tubulin, is a secondary factor affecting the value of  $IC_{50}$  and most of these compounds fall into a fairly narrow range due to a similar mode of binding to their target. On the other hand, SI is the ratio of the  $IC_{50}$ 's for normal cells versus cancer cells. It largely depends on the three main factors listed above of which solubility and membrane permeability do not change between cancer and normal cells, so it mainly depends on the affinity to P-gp, which is not known to us at present.

Therefore, we can see that the *in silico* results do not correlate with the *in vitro* determined biological activity of these compounds as indicated by the corresponding  $IC_{50}$  values. The inclusion

of binding affinity calculations for these compounds with regard to the other tubulin isotypes is still informative in a broader context of tubulin-binding agents and with respect to most important efflux transporters, in order to minimize interactions with the latter and maximize with the former, and hence increase the activity of the chemical compound.

Schematic interactions of the compounds with CBS residues of  $\beta$ I-tubulin are shown in Table 2 and Supplementary Materials Table S1. Derivatives 4–8 were designed with different alkyl chains at position C7 of 10-methylaminocolchicine 2. In this group, the common binding residues were Asn100, Leu688, Asn691, and Lys785. Compound 7 showed additionally some interactions with  $\alpha$ -tubulin (Gln10, Asn100, Ser177, Ala179). Another series with alkyl chains having various substituents (9–12) at C7 carbon were bound mostly through Asn100, Thr178, Leu681, Leu688, and Lys785. Compounds 13–17 have been designed with an aromatic group side chain without or with substituents at C7 position. The binding residues in this group belong to both  $\alpha$ -tubulin (Asn100, Thr178) and  $\beta$ -tubulin (Leu681, Asn682, Asp684, Leu688, Lys785).

**Table 2.** Computational predictions of interactions between starting compounds 1–3, most cytotoxic 14 and homology modeled tubulin  $\beta$ I. 3D representation and 2D layout of colchicine derivatives–tubulin protein complex, binding energy and active residues are tabulated.

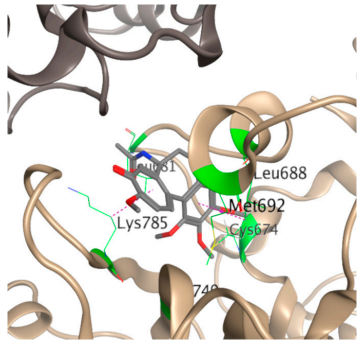
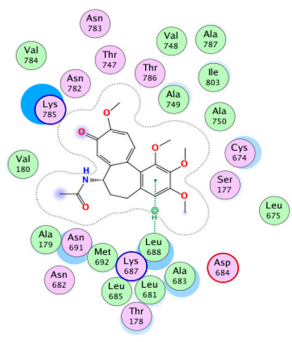
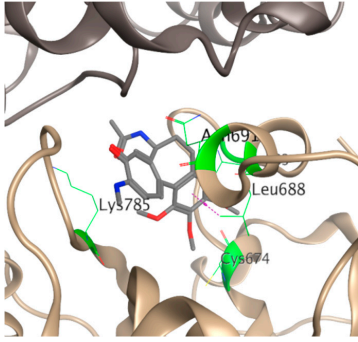
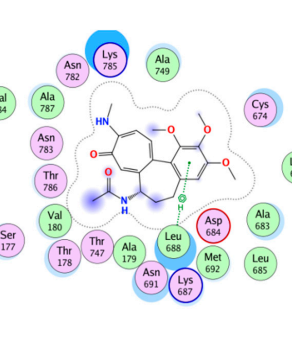
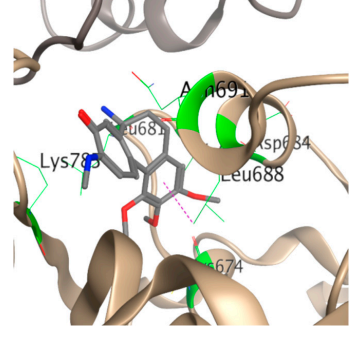
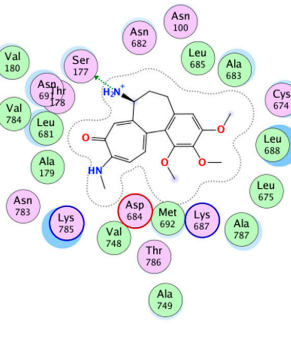
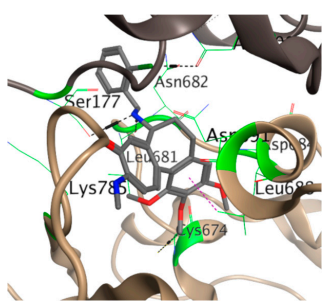
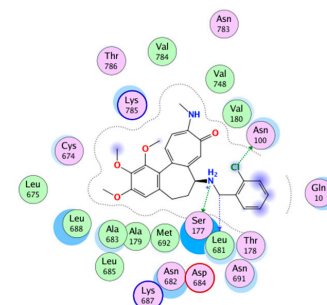
Compound	3D Representation of the Interactions	2D Representation of the Interactions	Binding Energy [kcal/mol]	Active Residues
1			−39.1	Cys674 Leu681 Ala683 Leu688 Met692 Ala749 Lys785
2			−37.5	Cys674 Ala683 Leu688 Asn691 Lys785
3			−4.5	Ser177 Cys674 Leu681 Ala683 Asp684 Leu688 Asn691 Lys785



Table 2. Cont.

Compound	3D Representation of the Interactions	2D Representation of the Interactions	Binding Energy [kcal/mol]	Active Residues
14			-31.5	<b>Asn100</b> <b>Ser177</b> <b>Cys674</b> <b>Leu681</b> <b>Asn682</b> <b>Asp684</b> <b>Leu688</b> <b>Lys785</b>
	<p> <span style="color: purple;">○</span> polar      <span style="color: green;">→</span> sidechain acceptor      <span style="border: 1px solid black; border-radius: 50%; padding: 2px;">○</span> solvent residue      <span style="border: 1px solid black; border-radius: 50%; padding: 2px;">⊗</span> arene-arene  <span style="color: red;">○</span> acidic      <span style="color: green;">←</span> sidechain donor      <span style="border: 1px solid black; border-radius: 50%; padding: 2px;">●</span> metal complex      <span style="border: 1px solid black; border-radius: 50%; padding: 2px;">⊗H</span> arene-H  <span style="color: blue;">○</span> basic      <span style="color: blue;">→</span> backbone acceptor      <span style="border: 1px solid black; border-radius: 50%; padding: 2px;">○</span> solvent contact      <span style="border: 1px solid black; border-radius: 50%; padding: 2px;">⊕</span> arene-cation  <span style="color: green;">○</span> greasy      <span style="color: blue;">←</span> backbone donor      <span style="border: 1px solid black; border-radius: 50%; padding: 2px;">○</span> metal/ion contact      <span style="border: 1px solid black; border-radius: 50%; padding: 2px;">○</span> receptor exposure  <span style="border: 1px solid black; border-radius: 50%; padding: 2px;">○</span> proximity contour      <span style="color: blue;">●</span> ligand exposure      <span style="border: 1px solid black; border-radius: 50%; padding: 2px;">○</span> receptor exposure </p>			

In 3D illustrations the interacting residues predicted from pairwise per-residue binding free energy decomposition calculations ( $E < -2$  kcal/mol) are shown in stick representation and their carbons and the ribbon are colored as green. Tubulin is shown in cartoon representation. Hydrogen bonds and their directionality are represented as black dashed arrows. The structures are color coded as follows: Tubulin  $\alpha$ I, brown; tubulin  $\beta$ I, beige. Ligands are displayed with stick and the atoms are colored as O (red), C (gray), N (blue), S (yellow), Cl (green), and F (pink). Binding energy defines the affinity of binding of colchicine derivatives complexed with tubulin  $\beta$ I. Binding energies are predicted by the MM/GBSA method. The last column contains information about active residues with binding free energy decomposition ( $E < -2$  kcal/mol) and the residues with ( $E < -3$  kcal/mol) are highlighted in bold. The last line contains the graphical key to help interpret the 2D part of the ligand interactions panel.

### 3. Materials and Methods

#### 3.1. General

Information concerning reagents and solvents can be found in the Supplementary Materials.

#### 3.2. Spectroscopic Measurements

Information concerning equipment used for measurements can be found in the Supplementary Materials.

#### 3.3. Synthesis

##### 3.3.1. Synthesis of **2** and **3**

Synthesis of 10-*N*-methylaminocolchicine **2** and *N*-deacetyl-10-methylamino-10-demethoxycolchicine **3** was performed according to the previously published procedure [20] and can be found in Supplementary Materials.

##### 3.3.2. General Procedure for the Synthesis of Colchicine Derivatives **5–9** and **12–17**

Compound **5–9** and **12–17** were obtained directly from compound **3**. To a solution of compound **3** (1.0 equiv.) in MeOH, the corresponding aldehyde (1.0 equiv.) was added followed in 15 min by  $\text{NaBH}_3\text{CN}$  (1.2 equiv.). Reaction progress was monitored by LC-MS. Then the mixture was evaporated under reduced pressure, diluted with EtOAc, washed with 5%  $\text{NaHCO}_3$  brine and dried over  $\text{Na}_2\text{SO}_4$ . The residue was purified using column flash chromatography (silica gel; EtOAc/MeOH, 20/1 v/v) and next lyophilized from dioxane to give respective compounds.

##### Compound **5**

Yellow solid, yield 47%.

ESI-MS for  $C_{23}H_{30}N_2O_4$  ( $m/z$ ):  $[M + H]^+$  399,  $[M + Na]^+$  421,  $[2M + H]^+$  797,  $[2M + Na]^+$  819.

$^1H$  NMR (500 MHz,  $CDCl_3$ )  $\delta$  7.64 (s, 1H), 7.36 (d,  $J = 11.0$  Hz, 1H), 7.27–7.25 (m, 1H), 6.53–6.48 (m, 2H), 3.91 (s, 3H), 3.88 (s, 3H), 3.55 (s, 3H), 3.41–3.37 (m, 1H), 3.06 (d,  $J = 5.4$  Hz, 3H), 2.51–2.47 (m, 1H), 2.45–2.35 (m, 1H), 2.33–2.27 (m, 1H), 2.24–2.15 (m, 2H), 1.72–1.65 (m, 1H), 1.46–1.37 (m, 2H), 0.82 (t,  $J = 7.4$  Hz, 3H).

$^{13}C$  NMR (126 MHz,  $CDCl_3$ )  $\delta$  175.7, 155.1, 152.6, 150.9, 150.6, 141.1, 138.6, 135.5, 130.5, 127.0, 124.4, 107.2, 107.1, 61.3, 61.0, 60.6, 56.1, 49.9, 39.4, 30.5, 29.5, 23.4, 11.8.

#### Compound 6

Yellow solid, yield 44%.

ESI-MS for  $C_{24}H_{32}N_2O_4$  ( $m/z$ ):  $[M + H]^+$  413,  $[M + Na]^+$  435,  $[2M + H]^+$  825,  $[2M + Na]^+$  847.

$^1H$  NMR (500 MHz,  $CDCl_3$ )  $\delta$  7.63 (s, 1H), 7.35 (d,  $J = 11.0$  Hz, 1H), 7.28–7.26 (s, 1H), 6.50–6.48 (d,  $J = 12.3$  Hz, 2H), 3.89 (s, 3H), 3.87 (s, 3H), 3.54 (s, 3H), 3.39–3.37 (m, 1H), 3.05 (d,  $J = 5.3$  Hz, 3H), 2.49–2.46 (m, 1H), 2.39–2.37 (m, 1H), 2.30–2.28 (m, 1H), 2.22–2.18 (m, 2H), 1.73–1.64 (m, 1H), 1.39–1.36 (m, 2H), 1.28–1.25 (m, 2H), 0.80 (t,  $J = 7.3$  Hz, 3H).

$^{13}C$  NMR (126 MHz,  $CDCl_3$ )  $\delta$  175.7, 155.1, 152.6, 150.7, 150.5, 141.1, 138.6, 135.5, 130.5, 126.9, 124.3, 107.3, 107.1, 61.3, 61.0, 60.6, 56.0, 47.6, 39.3, 32.3, 30.5, 29.5, 20.4, 14.0.

#### Compound 7

Yellow solid, yield 40%.

ESI-MS for  $C_{30}H_{44}N_2O_4$  ( $m/z$ ):  $[M + H]^+$  497,  $[M + Na]^+$  519,  $[2M + H]^+$  993,  $[2M + Na]^+$  1015.

$^1H$  NMR (500 MHz,  $CDCl_3$ )  $\delta$  7.64 (s, 1H), 7.36 (d,  $J = 11.1$  Hz, 1H), 7.32–7.27 (m, 1H), 6.52–6.48 (m, 2H), 3.90 (s, 3H), 3.87 (s, 3H), 3.55 (s, 3H), 3.44–3.37 (m, 1H), 3.06 (d,  $J = 5.4$  Hz, 3H), 2.55–2.48 (m, 1H), 2.43–2.37 (m, 1H), 2.34–2.26 (m, 1H), 2.25–2.17 (m, 2H), 1.75–1.67 (m, 1H), 1.44–1.36 (m, 2H), 1.26–1.15 (m, 14H), 0.83 (t,  $J = 7.0$  Hz, 3H).

$^{13}C$  NMR (126 MHz,  $CDCl_3$ )  $\delta$  175.6, 155.1, 152.7, 150.5, 141.1, 138.7, 135.4, 130.5, 126.9, 124.3, 107.3, 107.1, 61.3, 61.1, 60.6, 56.0, 48.0, 39.3, 31.9, 30.4, 29.6, 29.5, 29.3, 27.3, 22.7, 14.1.

#### Compound 8

Yellow solid, yield 45%.

ESI-MS for  $C_{24}H_{32}N_2O_4$  ( $m/z$ ):  $[M + H]^+$  413,  $[M + Na]^+$  435,  $[2M + H]^+$  825,  $[2M + Na]^+$  847.

$^1H$  NMR (500 MHz,  $CDCl_3$ )  $\delta$  7.68 (s, 1H), 7.36 (d,  $J = 11.0$  Hz, 1H), 7.25–7.21 (m, 1H), 6.55–6.47 (m, 2H), 3.92 (s, 3H), 3.89 (s, 3H), 3.56 (s, 3H), 3.38–3.34 (m, 1H), 3.07 (d,  $J = 5.4$  Hz, 3H), 2.42–2.38 (m, 1H), 2.33–2.29 (m, 2H), 2.24–2.15 (m, 1H), 2.08–2.04 (m, 1H), 1.73–1.68 (m, 1H), 1.64–1.62 (m, 1H), 0.88 (d,  $J = 6.6$  Hz, 3H), 0.82 (d,  $J = 6.6$  Hz, 3H).

$^{13}C$  NMR (126 MHz,  $CDCl_3$ )  $\delta$  175.8, 155.1, 152.6, 151.1, 150.6, 141.1, 138.5, 135.5, 130.5, 127.0, 124.6, 107.2, 107.0, 61.3, 61.2, 60.6, 56.0, 56.0, 39.4, 30.5, 29.5, 28.8, 20.8, 20.7.

#### Compound 9

Yellow solid, yield 50%.

ESI-MS for  $C_{22}H_{28}N_2O_5$  ( $m/z$ ):  $[M + H]^+$  401,  $[M + Na]^+$  423,  $[2M + H]^+$  801,  $[2M + Na]^+$  823.

$^1H$  NMR (500 MHz,  $CDCl_3$ )  $\delta$  7.62 (s, 1H), 7.39 (d,  $J = 11.1$  Hz, 1H), 7.35–7.33 (m, 1H), 6.57–6.50 (m, 2H), 3.90 (s, 3H), 3.88 (s, 3H), 3.64–3.57 (m, 2H), 3.55 (s, 3H), 3.48–3.44 (m, 1H), 3.13 (s, 1H), 3.07 (d,  $J = 5.4$  Hz, 3H), 2.7–2.74 (m, 1H), 2.45–2.40 (m, 2H), 2.35–2.25 (m, 2H), 1.75–1.71 (m, 1H).

$^{13}C$  NMR (126 MHz,  $CDCl_3$ )  $\delta$  175.4, 155.2, 152.8, 150.5, 150.4, 141.4, 139.1, 135.3, 130.7, 126.7, 124.0, 107.8, 107.2, 61.3, 61.2, 60.8, 60.7, 56.1, 49.6, 39.3, 30.4, 29.5.

#### Compound 12

Yellow solid, yield 55%.

ESI-MS for  $C_{23}H_{27}F_3N_2O_4$  ( $m/z$ ):  $[M + H]^+$  453,  $[M + Na]^+$  475,  $[2M + H]^+$  905,  $[2M + Na]^+$  927.

$^1H$  NMR (500 MHz,  $CDCl_3$ )  $\delta$  7.66 (s, 1H), 7.37 (d,  $J = 11.1$  Hz, 1H), 7.29–7.26 (m, 1H), 6.53–6.50 (m, 2H), 3.91 (s, 3H), 3.89 (s, 3H), 3.57 (s, 3H), 3.43–3.38 (m, 1H), 3.07 (d,  $J = 5.4$  Hz, 3H), 2.80–2.68 (m, 1H), 2.58–2.50 (m, 1H), 2.43–2.37 (m, 1H), 2.35–2.29 (m, 1H), 2.27–2.14 (m, 3H), 1.73–1.68 (m, 1H).

$^{13}C$  NMR (126 MHz,  $CDCl_3$ )  $\delta$  175.7, 155.1, 152.8, 150.6, 150.0, 141.2, 138.9, 135.3, 130.3, 127.7, 126.7, 124.0, 107.3, 107.1, 61.3, 60.9, 60.6, 56.0, 40.8, 40.8, 39.3, 30.4, 29.5.

### Compound 13

Yellow solid, yield 47%.

ESI-MS for  $C_{27}H_{30}N_2O_4$  ( $m/z$ ):  $[M + H]^+$  447,  $[M + Na]^+$  469,  $[2M + H]^+$  893,  $[2M + Na]^+$  915.

$^1H$  NMR (500 MHz,  $CDCl_3$ )  $\delta$  7.83 (s, 1H), 7.37 (d,  $J = 11.0$  Hz, 1H), 7.31–7.27 (m, 1H), 7.26–7.19 (m, 4H), 7.18–7.13 (m, 1H), 6.55–6.49 (m, 2H), 3.90 (s, 3H), 3.88 (s, 3H), 3.78–3.72 (m, 1H), 3.50 (s, 3H), 3.49–3.46 (m, 1H), 3.42–3.40 (m, 1H), 3.07 (d,  $J = 5.4$  Hz, 3H), 2.45–2.28 (m, 2H), 2.26–2.15 (m, 1H), 1.77–1.71 (m, 1H).

$^{13}C$  NMR (126 MHz,  $CDCl_3$ )  $\delta$  175.8, 155.1, 152.6, 150.6, 150.5, 141.1, 140.0, 138.7, 135.4, 130.5, 128.3, 128.2, 127.0, 126.9, 124.5, 107.2, 107.0, 61.3, 60.6, 60.4, 56.0, 51.9, 39.4, 30.5, 29.5.

### Compound 14

Yellow solid, yield 33%.

ESI-MS for  $C_{27}H_{29}ClN_2O_4$  ( $m/z$ ):  $[M + H]^+$  481/483,  $[M + Na]^+$  503,  $[2M + H]^+$  961,  $[2M + Na]^+$  983/985.

$^1H$  NMR (500 MHz,  $CDCl_3$ )  $\delta$  7.87 (s, 1H), 7.37 (d,  $J = 11.0$  Hz, 1H), 7.33 (dd,  $J = 7.2, 1.6$  Hz, 1H), 7.30–7.23 (m, 2H), 7.16–7.08 (m, 2H), 6.53–6.49 (m, 2H), 3.90 (s, 3H), 3.88 (s, 3H), 3.81–3.75 (m, 1H), 3.58–3.55 (m, 4H), 3.49–3.44 (m, 1H), 3.07 (d,  $J = 5.4$  Hz, 3H), 2.44–2.31 (m, 2H), 2.26–2.16 (m, 1H), 1.81–1.73 (m, 1H).

$^{13}C$  NMR (126 MHz,  $CDCl_3$ )  $\delta$  175.8, 155.1, 152.6, 150.6, 150.4, 141.1, 138.7, 137.4, 135.4, 133.6, 130.4, 130.2, 129.3, 128.3, 126.8, 124.6, 107.2, 107.0, 61.3, 60.7, 60.3, 56.0, 49.3, 39.3, 30.5, 29.5.

### Compound 15

Yellow solid, yield 51%.

ESI-MS for  $C_{27}H_{30}N_2O_5$  ( $m/z$ ):  $[M + H]^+$  463,  $[M + Na]^+$  485,  $[2M + H]^+$  925,  $[2M + Na]^+$  947,  $[M - H]^-$  461,  $[M + HCOO]^-$  507.

$^1H$  NMR (500 MHz,  $CDCl_3$ )  $\delta$  7.94 (s, 1H), 7.45 (d,  $J = 11.2$  Hz, 1H), 7.40–7.36 (m, 1H), 7.03 (d,  $J = 8.2$  Hz, 2H), 6.74 (d,  $J = 8.1$  Hz, 2H), 6.62 (d,  $J = 11.4$  Hz, 1H), 6.52 (s, 1H), 3.92 (s, 3H), 3.88 (s, 3H), 3.59–3.56 (m, 1H), 3.55 (s, 3H), 3.52–3.46 (m, 1H), 3.27 (d,  $J = 12.0$  Hz, 1H), 3.09 (d,  $J = 5.4$  Hz, 3H), 2.43–2.36 (m, 1H), 2.35–2.18 (m, 2H), 1.77–1.73 (m, 1H).

$^{13}C$  NMR (126 MHz,  $CDCl_3$ )  $\delta$  175.1, 156.4, 155.4, 152.8, 151.3, 150.6, 141.1, 139.6, 135.5, 131.4, 130.5, 129.5, 126.7, 124.2, 115.6, 108.6, 107.2, 61.4, 61.0, 60.8, 56.1, 51.8, 39.3, 30.5, 29.6.

### Compound 16

Yellow solid, yield 56%.

ESI-MS for  $C_{26}H_{29}N_3O_4$  ( $m/z$ ):  $[M + H]^+$  448,  $[M + Na]^+$  470,  $[2M + Na]^+$  917.

$^1H$  NMR (500 MHz,  $CD_3CN$ )  $\delta$  8.35 (d,  $J = 5.7$  Hz, 2H), 7.66 (s, 1H), 7.36–7.31 (m, 1H), 7.25 (d,  $J = 11.0$  Hz, 1H), 7.17 (d,  $J = 5.8$  Hz, 2H), 6.61 (s, 1H), 6.55 (d,  $J = 11.2$  Hz, 1H), 3.80 (s, 3H), 3.76 (s, 3H), 3.68 (d,  $J = 14.9$  Hz, 1H), 3.47 (d,  $J = 14.9$  Hz, 1H), 3.39 (s, 3H), 3.35–3.29 (m, 1H), 3.00 (d,  $J = 5.4$  Hz, 3H), 2.44–2.36 (m, 1H), 2.26–2.13 (m, 2H), 1.74–1.63 (m, 1H).

$^{13}C$  NMR (126 MHz,  $CD_3CN$ )  $\delta$  176.2, 156.1, 153.6, 151.3, 150.5, 150.4, 150.2, 141.9, 139.3, 136.2, 130.7, 127.5, 124.6, 123.9, 108.2, 107.7, 61.3, 61.0, 60.9, 56.5, 50.7, 39.5, 30.8, 29.7.

### Compound 17

Yellow solid, yield 40%.

ESI-MS for  $C_{25}H_{28}N_2O_4S$  ( $m/z$ ):  $[M + H]^+$  453,  $[M + Na]^+$  475,  $[2M + H]^+$  905,  $[2M + Na]^+$  927.

$^1H$  NMR (500 MHz,  $CDCl_3$ )  $\delta$  7.74 (s, 1H), 7.37 (d,  $J = 11.1$  Hz, 1H), 7.29–7.27 (m, 1H), 7.10 (dd,  $J = 5.0, 0.9$  Hz, 1H), 6.83–6.80 (m, 1H), 6.76 (d,  $J = 2.9$  Hz, 1H), 6.54–6.50 (m, 2H), 3.93 (d,  $J = 14.1$  Hz, 1H), 3.90 (s, 3H), 3.88 (s, 3H), 3.65 (d,  $J = 14.1$  Hz, 1H), 3.57–3.53 (m, 1H), 3.51 (s, 3H), 3.08 (d,  $J = 5.4$  Hz, 3H), 2.45–2.29 (m, 2H), 2.25–2.16 (m, 1H), 1.78–1.71 (m, 1H).

$^{13}C$  NMR (126 MHz,  $CDCl_3$ )  $\delta$  175.7, 155.1, 152.7, 150.6, 150.2, 143.8, 141.1, 138.8, 135.4, 130.5, 126.8, 126.5, 124.7, 124.4, 124.3, 107.3, 107.0, 61.3, 60.7, 59.9, 56.0, 46.3, 39.4, 30.5, 29.5.

### 3.3.3. General Procedure for the Synthesis of Colchicine Derivatives 4 and 11

Compound 4 and 11 were obtained in a two-step procedure. The first step involved the synthesis of aldehyde and the second was the reaction of the obtained aldehyde with the starting compound 3.

To a solution of appropriate alcohol (10.0 equiv.) in DCM was added PCC (30.0 equiv.) and the reaction mixture was stirred at RT for 4 h. After this time the mixture was filtered through thin pad of silica gel and the filtrate containing aldehyde was used in the next step (without further purification). To a solution of compound 3 (1.0 equiv.) in MeOH, one-second of the previously prepared portion of aldehyde was added followed in 15 min by  $NaBH_3CN$  (1.2 equiv.). After two hours, a further portion of the prepared aldehyde and  $NaBH_3CN$  (1.2 equiv.) were added. Reaction progress was monitored by LC-MS. Then the mixture was evaporated under reduced pressure, diluted with EtOAc, washed with 5%  $NaHCO_3$ , brine and dried over  $Na_2SO_4$ . The residue was purified using column flash chromatography (silica gel; DCM/MeOH, 30/1  $v/v$ ) and next lyophilized from dioxane to give respective compounds.

### Compound 4

Yellow solid, yield 13%.

ESI-MS for  $C_{22}H_{28}N_2O_4$  ( $m/z$ ):  $[M + H]^+$  385,  $[M + Na]^+$  407,  $[2M + Na]^+$  791.

$^1H$  NMR (500 MHz,  $CDCl_3$ )  $\delta$  7.77 (s, 1H), 7.43 (d,  $J = 11.1$  Hz, 1H), 7.26–7.24 (m, 1H), 6.64–6.53 (m, 2H), 3.93 (s, 3H), 3.91 (d,  $J = 4.6$  Hz, 3H), 3.90–3.84 (m, 1H), 3.60 (s, 3H), 3.12 (d,  $J = 5.3$  Hz, 3H), 2.86–2.69 (m, 1H), 2.59–2.30 (m, 4H), 1.87 (s, 1H), 1.13 (s, 3H).

### Compound 11

Yellow solid, yield 43%.

ESI-MS for  $C_{23}H_{29}N_2O_4$  ( $m/z$ ):  $[M + H]^+$  433/435,  $[M + Na]^+$  455/457,  $[2M + Na]^+$  887/889.

$^1H$  NMR (500 MHz,  $CD_2Cl_2$ )  $\delta$  7.59 (s, 1H), 7.33 (d,  $J = 11.0$  Hz, 1H), 7.25–7.22 (m, 1H), 6.59–6.47 (m, 2H), 3.86 (d,  $J = 1.9$  Hz, 6H), 3.62–3.55 (m, 2H), 3.54 (s, 3H), 3.38–3.36 (m, 1H), 3.06 (d,  $J = 5.5$  Hz, 3H), 2.63–2.60 (m, 1H), 2.50–2.39 (m, 2H), 2.31–2.29 (m, 1H), 2.26–2.16 (m, 1H), 1.87–1.82 (m, 2H), 1.74–1.65 (m, 1H).

$^{13}C$  NMR (126 MHz,  $CD_2Cl_2$ )  $\delta$  176.0, 155.5, 153.3, 151.1, 151.0, 141.7, 138.9, 135.9, 130.7, 127.3, 124.6, 107.6, 107.4, 61.5, 61.5, 60.9, 56.5, 45.4, 43.8, 39.8, 33.6, 30.8, 29.9.

### 3.3.4. Synthesis of 10

Compound 10 was obtained directly from compound 3. To a solution of compound 3 (1.0 equiv.) in MeOH, acrylonitrile (5.0 equiv.) was added. Reaction progress was monitored by LC-MS. Then the reaction mixture was diluted with EtOAc, washed with 5%  $NaHCO_3$ , brine and dried over  $Na_2SO_4$ . The residue was purified using column flash chromatography (silica gel; DCM/MeOH) and next lyophilized from dioxane to give the pure product 10 as a yellow solid with a yield of 19%.

ESI-MS for  $C_{23}H_{27}N_3O_4$  ( $m/z$ ):  $[M + H]^+$  410,  $[M + Na]^+$  432,  $[2M + Na]^+$  841,  $[M - H]^-$  408,  $[M + HCOO]^-$  454.

$^1\text{H}$  NMR (500 MHz,  $\text{CDCl}_3$ )  $\delta$  7.63 (s, 1H), 7.39 (d,  $J = 11.1$  Hz, 1H), 7.3–7.27 (m, 1H), 6.60–6.49 (m, 2H), 3.92 (s, 3H), 3.91 (s, 3H), 3.59 (s, 3H), 3.51–3.40 (m, 1H), 3.09 (d,  $J = 5.4$  Hz, 3H), 2.84–2.80 (m, 1H), 2.68–2.57 (m, 1H), 2.49–2.40 (m, 3H), 2.36–2.30 (m, 1H), 2.28–2.21 (m, 1H), 1.77–1.71 (m, 1H).

### 3.4. In Vitro Antiproliferative Activity

Cytotoxic activity was tested according to the previously published procedure [20] and detailed information can be found in Supplementary Materials.

### 3.5. Molecular Docking Studies

Molecular docking studies was performed according to the previously published procedure [20] and detailed information can be found in Supplementary Materials.

## 4. Conclusions

In summary, a series of novel double-modified colchicine analogues derivatized at their C7 (single carbon-nitrogen bond) and C10 (methylamino substituent) positions, were devised. All compounds were successfully synthesized, purified and their structures were confirmed by spectroscopic analyses. All target compounds were screened for their in vitro cytotoxicity against A549, MCF-7, LoVo, and LoVo/DX cells to evaluate their anticancer potency.

All presented derivatives were shown to be active at nanomolar concentrations and exhibited better antiproliferative activity than the commonly used anticancer agents doxorubicin and cisplatin. The introduction of methylamino group at position C10 significantly increased the cytotoxicity of a relevant derivative in comparison to that of unmodified colchicine **1**. In addition, the majority of the investigated double-modified derivatives exhibited excellent potency ( $\text{IC}_{50} \leq 10$  nM) against A549, MCF-7, LoVo cell lines. The most toxic to all tumor cells tested was derivative **14** with 2-chlorobenzyl moiety at C7 carbon ( $\text{IC}_{50} = 0.1$ – $1.6$  nM). Thus, preliminary conclusions revealed that the choice of the type of chemical bond or substituent at C7 and C10 positions was critical for the cytotoxicity of the compounds.

The calculated values of resistance index (RI) indicated that colchicine-based compounds can be effective against drug-resistant cancer cells. Eleven new derivatives (**3–8**, **11–13**, **16–17**) showed  $\text{RI} \leq 10$ , which means that LoVo/DX cells are sensitive to these compounds. Although these compounds have low RI values, they have proved to be non-selective for cancer cells in relation to normal cells (low SI values). Further evaluation should help to find more detailed structure–activity relationships for the drugs overcoming the resistance of tumor cells, which can help in rational drug design efforts in future. In terms of selectivity for cancerous versus normal cells, only one derivative **14** was superior to parent amides **1** and **2**. Replacement of acetyl at C7 carbon with a 2-chlorobenzyl moiety and simultaneous substitution of methoxy group to methylamino group at position C10 allowed obtaining a compound selective towards all four cancer cell lines tested (high SI values from 2.8 to 93.7).

Molecular docking studies showed that apart from the initial amides **1** and **2**, compound **14**, which had the best antiproliferative activity, stood out also in terms of its predicted binding energy and probably binds best into the active site of  $\beta\text{I}$ -tubulin isotype. Otherwise, no correlation between in vitro and *in silico* results was observed indicating that other factors than affinity to the target determine their biological activity. These factors may include solubility, membrane permeability as well as off-target interactions including the affinity to P-glycoprotein.

Derivative **14** with strong in vitro antiproliferative activity and high SI values, represents the most promising lead for further development. Test results for this compound are noteworthy and suggest that extended and more detail in vivo research of **14** and similar derivatives is necessary to determine their therapeutic potential as anticancer drugs.

**Supplementary Materials:** The following are available online, Table S1: Computational predictions of interactions between tested compounds (**1–17**) and homology modeled tubulin  $\beta\text{I}$ , Figure S1: The LC-MS chromatogram

and mass spectra of **2**, Figure S2: The  $^1\text{H}$  NMR spectrum of **2** in  $\text{CDCl}_3$ , Figure S3: The  $^{13}\text{C}$  NMR spectrum of **2** in  $\text{CDCl}_3$ , Figure S4: The LC-MS chromatogram and mass spectra of **3**, Figure S5: The  $^1\text{H}$  NMR spectrum of **3** in  $\text{CDCl}_3$ , Figure S6: The  $^{13}\text{C}$  NMR spectrum of **3** in  $\text{CDCl}_3$ , Figure S7: The LC-MS chromatogram and mass spectra of **4**, Figure S8: The LC-MS chromatogram and mass spectra of **5**, Figure S9: The  $^1\text{H}$  NMR spectrum of **5** in  $\text{CDCl}_3$ , Figure S10: The  $^{13}\text{C}$  NMR spectrum of **5** in  $\text{CDCl}_3$ , Figure S11: The LC-MS chromatogram and mass spectra of **6**, Figure S12: The  $^1\text{H}$  NMR spectrum of **6** in  $\text{CDCl}_3$ , Figure S13: The  $^{13}\text{C}$  NMR spectrum of **6** in  $\text{CDCl}_3$ , Figure S14: The LC-MS chromatogram and mass spectra of **7**, Figure S15: The  $^1\text{H}$  NMR spectrum of **7** in  $\text{CDCl}_3$ , Figure S16: The  $^{13}\text{C}$  NMR spectrum of **7** in  $\text{CDCl}_3$ , Figure S17: The LC-MS chromatogram and mass spectra of **8**, Figure S18: The  $^1\text{H}$  NMR spectrum of **8** in  $\text{CDCl}_3$ , Figure S19: The  $^{13}\text{C}$  NMR spectrum of **8** in  $\text{CDCl}_3$ , Figure S20: The LC-MS chromatogram and mass spectra of **9**, Figure S21: The  $^1\text{H}$  NMR spectrum of **9** in  $\text{CDCl}_3$ , Figure S22: The  $^{13}\text{C}$  NMR spectrum of **9** in  $\text{CDCl}_3$ , Figure S23: The LC-MS chromatogram and mass spectra of **10**, Figure S24: The  $^1\text{H}$  NMR spectrum of **10** in  $\text{CDCl}_3$ , Figure S25: The LC-MS chromatogram and mass spectra of **11**, Figure S26: The  $^1\text{H}$  NMR spectrum of **11** in  $\text{CD}_2\text{Cl}_2$ , Figure S27: The  $^{13}\text{C}$  NMR spectrum of **11** in  $\text{CD}_2\text{Cl}_2$ , Figure S28: The LC-MS chromatogram and mass spectra of **12**, Figure S29: The  $^1\text{H}$  NMR spectrum of **12** in  $\text{CDCl}_3$ , Figure S30: The  $^{13}\text{C}$  NMR spectrum of **12** in  $\text{CDCl}_3$ , Figure S31: The LC-MS chromatogram and mass spectra of **13**, Figure S32: The  $^1\text{H}$  NMR spectrum of **13** in  $\text{CDCl}_3$ , Figure S33: The  $^{13}\text{C}$  NMR spectrum of **13** in  $\text{CDCl}_3$ , Figure S34: The LC-MS chromatogram and mass spectra of **14**, Figure S35: The  $^1\text{H}$  NMR spectrum of **14** in  $\text{CDCl}_3$ , Figure S36: The  $^{13}\text{C}$  NMR spectrum of **14** in  $\text{CDCl}_3$ , Figure S37: The LC-MS chromatogram and mass spectra of **15**, Figure S38: The  $^1\text{H}$  NMR spectrum of **15** in  $\text{CDCl}_3$ , Figure S39: The  $^{13}\text{C}$  NMR spectrum of **15** in  $\text{CDCl}_3$ , Figure S40: The LC-MS chromatogram and mass spectra of **16**, Figure S41: The  $^1\text{H}$  NMR spectrum of **16** in  $\text{CD}_3\text{CN}$ , Figure S42: The  $^{13}\text{C}$  NMR spectrum of **16** in  $\text{CD}_3\text{CN}$ , Figure S43: The LC-MS chromatogram and mass spectra of **17**, Figure S44: The  $^1\text{H}$  NMR spectrum of **17** in  $\text{CDCl}_3$ , Figure S45: The  $^{13}\text{C}$  NMR spectrum of **17** in  $\text{CDCl}_3$ .

**Author Contributions:** Conceptualization, J.K. and A.H.; methodology, J.K., A.H., J.W. and J.A.T.; software, M.A.; validation, A.H. and J.A.T.; formal analysis, A.H. and J.K.; investigation, J.K., E.M. and M.A.; resources, A.H.; J.K. and W.M.; data curation, J.K., M.A. and E.M.; writing—original draft preparation, J.K. and M.A.; writing—review and editing, W.M., A.H., J.W. and J.A.T.; visualization, J.K. and M.A.; supervision, A.H.; project administration, A.H.; funding acquisition, A.H. and W.M. All authors have read and agreed to the published version of the manuscript.

**Funding:** This research received no external funding.

**Conflicts of Interest:** The authors declare no conflict of interest.

## References

1. Wood, K.W.; Cornwell, W.D.; Jackson, J.R. Past and future of the mitotic spindle as an oncology target. *Curr. Opin. Pharmacol.* **2001**, *1*, 370–377. [[CrossRef](#)]
2. Vindya, N.G.; Sharma, N.; Yadav, M.; Ethiraj, K.R. Tubulins—The Target for Anticancer Therapy. *Curr. Top. Med. Chem.* **2015**, *15*, 73–82. [[CrossRef](#)] [[PubMed](#)]
3. Moscow, J.A.; Cowan, K.H. Multidrug Resistance. *J. Natl. Cancer Inst.* **1988**, *80*, 14–20. [[CrossRef](#)] [[PubMed](#)]
4. Druley, T.E.; Stein, W.D.; Ruth, A.; Roninson, I.B. P-glycoprotein-mediated colchicine resistance in different cell lines correlates with the effects of colchicine on P-glycoprotein conformation. *Biochemistry* **2001**, *40*, 4323–4331. [[CrossRef](#)] [[PubMed](#)]
5. Szakács, G.; Paterson, J.K.; Ludwig, J.A.; Booth-Genthe, C.; Gottesman, M.M. Targeting multidrug resistance in cancer. *Nat. Rev. Drug Discov.* **2006**, *5*, 219–234. [[CrossRef](#)] [[PubMed](#)]
6. Capraro, H.G.; Brossi, A. Chapter 1 Tropolonic Colchicum Alkaloids. *Alkaloids Chem. Pharmacol.* **1984**, *23*, 1–70.
7. Boyé, O.; Brossi, A. Tropolonic Colchicum Alkaloids and Allo Congeners. *Alkaloids Chem. Pharmacol.* **1992**, *41*, 125–176.
8. Hastie, S.B. Interactions of colchicine with tubulin. *Pharmacol. Ther.* **1991**, *51*, 377–401. [[CrossRef](#)]
9. Sapra, S.; Bhalla, Y.; Nandani, S.; Sharma, S.; Singh, G.; Nepali, K.; Budhiraja, A.; Dhar, K.L. Colchicine and its various physicochemical and biological aspects. *Med. Chem. Res.* **2013**, *22*, 531–547. [[CrossRef](#)]
10. Skoufias, D.A.; Wilson, L. Mechanism of Inhibition of Microtubule Polymerization by Colchicine: Inhibitory Potencies of Unliganded Colchicine and Tubulin-Colchicine Complexes. *Biochemistry* **1992**, *31*, 738–746. [[CrossRef](#)]
11. Bhattacharyya, B.; Panda, D.; Gupta, S.; Banerjee, M. Anti-mitotic activity of colchicine and the structural basis for its interaction with tubulin. *Med. Res. Rev.* **2008**, *28*, 155–183. [[CrossRef](#)] [[PubMed](#)]



12. Ravelli, R.B.G.; Gigant, B.; Curmi, P.A.; Jourdain, I.; Lachkar, S.; Sobel, A.; Knossow, M. Insight into tubulin regulation from a complex with colchicine and a stathmin-like domain. *Nature* **2004**, *428*, 198–202. [[CrossRef](#)] [[PubMed](#)]
13. Wiesenfeld, P.L.; Garthoff, L.H.; Sobotka, T.J.; Suagee, J.K.; Barton, C.N. Acute oral toxicity of colchicine in rats: Effects of gender, vehicle matrix and pre-exposure to lipopolysaccharide. *J. Appl. Toxicol.* **2007**, *27*, 421–433. [[CrossRef](#)] [[PubMed](#)]
14. Spiller, H.A. Colchicine. In *Encyclopedia of Toxicology: Third Edition*; Wexler, P., Ed.; Elsevier Inc.: London, UK, 2014; pp. 1007–1008. ISBN 9780123864543.
15. Roubille, F.; Kritikou, E.; Busseuil, D.; Barrere-Lemaire, S.; Tardif, J.-C. Colchicine: An Old Wine in a New Bottle? *Antiinflamm. Antiallergy Agents Med. Chem.* **2013**, *12*, 14–23. [[CrossRef](#)]
16. Mendis, S. Colchicine cardiotoxicity following ingestion of *Gloriosa superba* tubers. *Postgrad. Med. J.* **1989**, *65*, 752–755. [[CrossRef](#)]
17. Margolis, R.L.; Wilson, L. Addition of colchicine tubulin complex to microtubule ends: The mechanism of substoichiometric colchicine poisoning. *Proc. Natl. Acad. Sci. USA* **1977**, *74*, 3466–3470. [[CrossRef](#)]
18. Kuncl, R.W.; Duncan, G.; Watson, D.; Alderson, K.; Rogawski, M.A.; Peper, M. Colchicine Myopathy and Neuropathy. *N. Engl. J. Med.* **1987**, *316*, 1562–1568. [[CrossRef](#)]
19. Finkelstein, Y.; Aks, S.E.; Hutson, J.R.; Juurlink, D.N.; Nguyen, P.; Dubnov-Raz, G.; Pollak, U.; Koren, G.; Bentur, Y. Colchicine poisoning: The dark side of an ancient drug. *Clin. Toxicol.* **2010**, *48*, 407–414. [[CrossRef](#)]
20. Krzywik, J.; Mozga, W.; Aminpour, M.; Janczak, J.; Maj, E.; Wietrzyk, J.; Tuszyński, J.A.; Huczyński, A. Synthesis, antiproliferative activity and molecular docking studies of novel doubly modified colchicine amides and sulfonamides as anticancer agents. *Molecules* **2020**, *25*, 1789. [[CrossRef](#)]
21. Kerekes, P.; Sharma, P.N.; Brossi, A.; Chignell, C.F.; Quinn, F.R. Synthesis and Biological Effects of Novel Thiocolchicines. 3. Evaluation of *N*-Acyldeacetylthiocolchicines, *N*-(Alkoxy carbonyl)deacetylthiocolchicines, and *O*-Ethyl demethylthiocolchicines. New Synthesis of Thiodemecolcine and Antileukemic Effects of 2-Demeth. *J. Med. Chem.* **1985**, *28*, 1204–1208. [[CrossRef](#)]
22. Sun, L.; Hamel, E.; Lin, C.M.; Hastie, S.B.; Pyluck, A.; Lee, K.H. Antitumor Agents. 141. Synthesis and Biological Evaluation of Novel Thiocolchicine Analogs: *N*-Acyl-, *N*-Aroyl-, and *N*-(Substituted benzyl)deacetylthiocolchicines as Potent Cytotoxic and Antimitotic Compounds. *J. Med. Chem.* **1993**, *36*, 1474–1479. [[CrossRef](#)] [[PubMed](#)]
23. Gelmi, M.L.; Mottadelli, S.; Pocar, D.; Riva, A.; Bombardelli, E.; De Vincenzo, R.; Scambia, G. *N*-deacetyl-*N*-aminoacylthiocolchicine derivatives: Synthesis and biological evaluation on MDR-positive and MDR-negative human cancer cell lines. *J. Med. Chem.* **1999**, *42*, 5272–5276. [[CrossRef](#)] [[PubMed](#)]
24. Lee, S.H.; Park, S.K.; Kim, J.M.; Kim, M.H.; Kim, K.H.; Chun, K.W.; Cho, K.H.; Youn, J.Y.; Namgoong, S.K. New synthetic thiocolchicine derivatives as low-toxic anticancer agents. *Arch. Pharm. (Weinheim)* **2005**, *338*, 582–589. [[CrossRef](#)] [[PubMed](#)]
25. Marzo-Mas, A.; Barbier, P.; Breuzard, G.; Allegro, D.; Falomir, E.; Murga, J.; Carda, M.; Peyrot, V.; Marco, J.A. Interactions of long-chain homologues of colchicine with tubulin. *Eur. J. Med. Chem.* **2017**, *126*, 526–535. [[CrossRef](#)]
26. Majcher, U.; Urbaniak, A.; Maj, E.; Moshari, M.; Delgado, M.; Wietrzyk, J.; Bartl, F.; Chambers, T.C.; Tuszyński, J.A.; Huczyński, A. Synthesis, antiproliferative activity and molecular docking of thiocolchicine urethanes. *Bioorg. Chem.* **2018**, *81*, 553–566. [[CrossRef](#)]
27. Marzo-Mas, A.; Falomir, E.; Murga, J.; Carda, M.; Marco, J.A. Effects on tubulin polymerization and down-regulation of c-Myc, hTERT and VEGF genes by colchicine haloacetyl and haloaroyl derivatives. *Eur. J. Med. Chem.* **2018**, *150*, 591–600. [[CrossRef](#)]
28. Testa, B.; Mayer, J.M. *Hydrolysis in Drug and Prodrug Metabolism: Chemistry, Biochemistry, and Enzymology*; Verlag Helvetica Chimica Acta: Zürich, Switzerland, 2006; ISBN 9783906390444.
29. Rautio, J.; Kumpulainen, H.; Heimbach, T.; Oliyai, R.; Oh, D.; Järvinen, T.; Savolainen, J. Prodrugs: Design and clinical applications. *Nat. Rev. Drug Discov.* **2008**, *7*, 255–270. [[CrossRef](#)]
30. Cosentino, L.; Redondo-Horcajo, M.; Zhao, Y.; Santos, A.R.; Chowdury, K.F.; Vinader, V.; Abdallah, Q.M.A.; Abdel-Rahman, H.; Fournier-Dit-Chabert, J.; Shnyder, S.D.; et al. Synthesis and biological evaluation of colchicine B-ring analogues tethered with halogenated benzyl moieties. *J. Med. Chem.* **2012**, *55*, 11062–11066.
31. Kiyoshi, A. *N*-Methyldeacetylcolchicineamide Derivatives. Patent EP0607647(A1), 27 July 1994.

32. Corey, E.J.; Suggs, J.W. Pyridinium chlorochromate. An efficient reagent for oxidation of primary and secondary alcohols to carbonyl compounds. *Tetrahedron Lett.* **1975**, *16*, 2647–2650. [[CrossRef](#)]
33. Tateishi, T.; Soucek, P.; Caraco, Y.; Peter Gnengerich, F.; Wood, A.J.J. Colchicine biotransformation by human liver microsomes. *Biochem. Pharmacol.* **1997**, *53*, 111–116. [[CrossRef](#)]
34. Niel, E.; Scherrmann, J.M. Colchicine today. *Jt. Bone Spine* **2006**, *73*, 672–678. [[CrossRef](#)] [[PubMed](#)]

**Sample Availability:** Samples of the compounds are not available from the authors.



© 2020 by the authors. Licensee MDPI, Basel, Switzerland. This article is an open access article distributed under the terms and conditions of the Creative Commons Attribution (CC BY) license (<http://creativecommons.org/licenses/by/4.0/>).